RSC Advances

ROYAL SOCIETY OF CHEMISTRY

www.rsc.org/advances

Synthesis of phenolic amide as evaluation antioxidative and anti-inflammatory *in vitro* and *in vivo*

Ya-Ting Lee[1], You-Liang Hsieh[2] , Yen-Hung Yeh[3,4*], Chih-Yang Huang[2,5,6]

1. Department of Beauty Science, National Taichung University of Science and Technology, Taichung, Taiwan, R.O.C.

2. Department of Health and Nutrition Biotechnology, Asia University, Taichung, Taiwan, R.O.C.

3. School of Health Diet and Industry Management, Chung Shan Medical University, Taichung, Taiwan, R.O.C.

4. Department of Nutrition, Chung Shan Medical University Hospital, Taichung, Taiwan, R.O.C.

5. Graduate Institute of Basic Medical Science, China Medical University, Taichung, Taiwan, R.O.C.

6. Department of Chinese Medicine, China Medical University Hospital, Taichung, Taiwan, R.O.C.

Running title: Phenolic acid, phenolic amide, antioxidative agents, free radical scavenging

Corresponding author:

* Corresponding author. Tel.: +886-4-24730022

E-mail address: yhyeh@csmu.edu.tw (Y. H. Yeh).

Abstract

A series of 15 phenolic amides (PAs) have been synthesized (PA1-PA15) was examined *in vitro* by four different tests: 1. Preventing Cu^{2+}-induced human low-density lipoprotein oxidation. 2. Scavenging the stable radical. 3. Anti-inflammatory activity. 4. Scavenging of superoxide radicals. We used PA1 and α-tocopherol *in vivo* study. The overall potential of the antioxidant system was significantly enhanced by the PA1 and α-tocopherol supplements as the hepatic TBARS levels were lowered while the hepatic SOD activities and GSH concentration were elevated in PA1 fed rats. Our results supported PA1 may exert antioxidative action through inhibiting superoxide generations. PA1 decreased the level of nitric oxide (NO) production, tumor necrosis factor-alpha (TNF-α) and nuclear factor-kappa B (NF-κB). These results point out that PA1 can inhibit lipid peroxidation, enhance the activities of antioxidant enzymes, and decrease the TNF-α/NF-κB level, nitric oxide production. Therefore, it was speculated that PA1 through its anti-inflammation capacity.

Key words: Phenolic amides, antioxidative, free radical scavenging, superoxide, anti-inflammatory

1. Introduction

Oxidative stress is a contributing factor to the pathogenesis of neurodegenerative disorders such as cerebral ischemia/ reperfusion injury and trauma as well as chronic conditions such as Parkinson's disease and Alzheimer's disease [1]. Metabolism of oxygen in living cells leads to oxygen-derived free radicals production [2]. These free radicals attack the unsaturated fatty acids of biomembranes, which results in the destruction of proteins and DNA and lipid peroxidation [3]. Thus, the development of antioxidants, which can retard the process of lipid peroxidation by blocking the production of free radical chain reaction, has gained importance in recent years [4].

Phenolic acid derivatives are widely distributed in plants [5] but there only a few phenolic amides. The pharmacological functionality of phenolic amides have attracted much attention and have been acknowledged as having interesting medicinal properties, such as anti-inflammatory, antiviral, anti-cancer and anti-coagulant activities [6-8]. Recently, we found *N-trans*- and *N-cis*-feruloyl 3-methyldopamine in *Achyranthes bidentata*, a famous Chinese herb for many diseases. *Achyranthes bidentata* is an erect, annual herb distributed in hilly districts of India, Java, China and Japan. The plant is used in indigenous system of medicine as emenagogue, antiarthritic, antifertility, laxative, ecbolic, abortifacient, anthelmintic, aphrodisiac, antiviral, antispasmodic, antihypertensive, anticoagulant, diuretic and antitumour [9]. Also it is useful to treat cough, renal dropsy, fistula, scrofula, skin rash, nasal infection, chronic malaria, impotence, fever, asthma, amennorrhoea, piles, abdominal cramps and snake bites. The analysis of phytochemical profile revealed that it contains rutin, saponins, achyranthine, caffeic acid, oleanolic acid, inokosterone, ecdysterone, rubrosterone and physcion [10]. This put us to synthesize more phenolic amides for optimizing its antioxidative activity. In this study, the antioxidative activities were

examined by four different tests: We evaluated the antioxidant activities on the inhibition of Cu^{2+}-induced human LDL oxidation was chosen at the in vitro assay system, the radical scavenging activity against stable radical 1,1-diphenyl-2-picrylhydrazyl (DPPH), oxygen radical absorbance capacity (ORAC) assay and inhibition of superoxide production in the xanthine/xanthine oxidase (X/XO) system as well as evaluation the effect on the stimulus-induced superoxide generation in human neutrophil.

These activated macrophages released inflammatory mediators including tumor necrosis factor-alpha (TNF-α)/nuclear factor-kappa B (NF-κB), and nitric oxide (NO) that have been implicated in liver damage induced by a number of different toxicants [11].

Hence, the present study was undertaken to investigate the antioxidative and anti-inflammatory activities of PA1 in comparison α-tocopherol, in male Sprague-Dawley rats.

2. Materials and methods

2.1. Materials

Chemicals and reagents: 2-hydroxycinnamic acid (97%), 3-hydroxycinnamic acid (99%), 4-hydroxycinnamic acid (99%), ferulic acid (99%), isoferulic acid (97%), 3-hydroxytyramine hydrochloride, 3-methyldopamine hydrochloride and 4-methyldopamine hydrochloride, 2,2-Azobis(2-methylproprionamidine) dihydrochloride (AAPH), fluorescein disodium and 6-hydroxy-2,5,7,8-tetramethylchroman-2-carboxylic acid (Trolox) were purchased from Aldrich-Sigma Chemical Co (St. Louis, MO, USA). 1,3-dicyclohexylcarbodiimid, Benzyl chloride, Trichlorobromide, Methyl iodide,

Phenethyl alcohol, α-tocopherol were purchased from Riedel-de Haën Chemical Co (St. Louis, MO, USA). Copper sulfate pentahydrate, ethylenediaminetetraacetic acid (EDTA), potassium dihydrogen phosphate, sodium chloride, sodium bromide, di-sodium hydrogen phosphate ethanol and cholesterin enzymatic CHOD-RAP method (code no. 1.14366.0001) were purchased from E. Merck Chemical Co (Darmstadt, Germany). Lipofilm (code no. 4040-2) was purchased from Sebia Co. Phorbol 12-myristate 13-acetate (PMA) (99%), *N*-formyl-methionyl-leucyl-phenyl-alanine (fMLP) (99%), bis-*N*-methylacridinium nitrate (lucigenin), xanthine (99%) and xanthine oxidase were purchased from Aldrich-Sigma Chemical Co (St. Louis, MO, USA). General Synthetic Procedure for Phenolic Amides: The phenolic amides (PA1-PA15) were prepared from condensation of the corresponding phenolic acids (1.0 mmol) and phenethylamines (1.1 mmol) with the substitution by hydroxy and/or methoxy groups on the phenyl rings in the presence of DCC (4.0 mmol). The reaction mixture was stirred in THF overnight at room temperature. After removal of the solvent of the reaction mixture, water was added and extracted with EtOAc. The EtOAc layer was dried over Na_2SO_4 and evap'd to dryness, which was purified by a column of silical gel ($CHCl_3$-Me_2CO, 10:1) to afford the final product. The over yield was about 30-62%. Structures were confirmed with infrared, nuclear magnetic resonance and high resolution mass spectrometry (Table 1).

2.2. Analytical and Spectral Equipment

Synthesized products were purified on a silical gel column and identified by Thin layer chromatography (TLC), Nuclear magnetic resonance (NMR), Infrared spectra (IR) and GC Mass analysis. Melting points (Mp) were determined with a Yanaco

micromelting point apparatus. IR were obtained on a Nicolet Avatar-320 FTIR spectrophotometer. NMR spectra were recorded on a Varian INOVA-500 spectrometer. $CDCl_3$, CD_3OD and acetone-d_6 were used as solvents; chemical shifts are reported in parts per million (δ) units relative to internal tetramethylsilane. Mass spectra (MS) were recorded on an EI-MS JEOL JMS-HX 100 mass spectrometer. TLC was performed on precoated silical gel F254 plates (Merck) using a 254 nm UV lamp to monitor these reactions.

2.3. Identification of the PAs (PA1-PA15)

N-trans-O-coumaroyldopamine (PA1): Colorless oil; yield 35%. IR (film) $_{max}$ 3400, 1650, 1600, 1510, 1200/cm. ^{1}H-NMR (acetone-d_6): δ2.72 (2H, t, J = 7.0 Hz), 3.56 (2H, m), 6.56 (1H, dd, J = 2.0, 8.0 Hz), 6.74 (1H, d, J = 8.0 Hz), 6.78 (1H, d, J = 2.0 Hz), 6.79 (1H, d, J = 16.0 Hz), 6.83 (1H, m), 6.97 (1H, dd, J = 2.0, 8.0 Hz), 7.17 (1H, m), 7.46 (1H, dd, J = 2.0, 8.0 Hz), 7.63 (1H, t, -NH), 7.96 (1H, d, J = 16.0 Hz). HREIMS *m/z* 299.1160 (calcd for $C_{17}H_{17}NO_4$, 299.1158).

N-trans-m-coumaroyldopamine (PA2): Colorless oil; yield 40%. IR (film) $_{max}$ 3400, 1610, 1500, 1200/cm. ^{1}H-NMR(acetone-d_6): δ2.71 (2H, t, J = 7.2 Hz), 3.51 (2H, m), 6.56 (1H, dd, J = 8.0, 2.0 Hz), 6.76 (1H, dd, J = 8.0, 2.0 Hz), 6.85 (1H, m), 7.02 (1H, d, J = 15.8 Hz), 7.03 (1H, d, J = 2.0 Hz), 7.19 (1H, *t,* -NH), 7.51 (1H, d, J = 15.8 Hz). HREIMS *m/z* 299.1166 (calcd for $C_{17}H_{17}NO_4$, 299.1158).

N-trans-feruloyldopamine (PA3): Colorless oil; yield 48%. IR (film) $_{max}$ 3400, 1650, 1600, 1515, 1200/cm. ^{1}H-NMR(Acetone-d_6): δ2.69 (2H, t, J = 7.0 Hz), 3.48 (2H, q, J = 7.0 Hz), 3.85 (3H, s, -OCH_3), 6.51 (1H, d, J =15.5 Hz), 6.55 (1H, dd, J = 8.0, 2.0 Hz), 6.73 (1H, d, J = 8.0 Hz), 6.73 (1H, d, J = 2.0 Hz), 6.82 (1H, d, J = 8.0 Hz), 7.02 (1H, dd, J = 8.0, 2.0 Hz), 7.14 (1H, d, J = 2.0 Hz), 7.28 (t, br, -NH), 7.45

(1H, d, J = 15.5 Hz). HREIMS *m/z* 329.1261 (calcd for $C_{18}H_{19}NO_5$, 329.1263).

N-trans-p-coumaroyldopamine (PA4): Colorless oil; yield 31%. IR (film) $_{max}$ 3400, 1650, 1600, 1515, 1210/cm. ^{1}H-NMR(acetone-d_6): δ 2.69 (1H, t, J = 7.3 Hz), 3.49 (3H, m), 6.50 (1H, d, J = 15.7 Hz), 6.55 (2H, dd, J = 8.0, 2.0 Hz), 6.85 (2H, dd, J = 8.0, 2.0 Hz), 7.40 (2H, m), 7.49 (1H, d, J = 15.7 Hz). HREIMS *m/z* 299.1154 (calcd for $C_{17}H_{17}NO_4$, 299.1158).

N-trans-feruloyl-3-methyldopamine (PA5): White solid; Mp 154-157℃; yield 58%. IR (KBr) $_{max}$ 3400, 1650, 1520, 1210, 1100/cm. ^{1}H-NMR (acetone-d_6): δ2.75 (2H, t, J = 7.0 Hz), 3.50 (2H, q, J = 7.0 Hz), 3.81 (3H, s), 3.87 (3H, s), 6.49 (1H, d, J = 15.5 Hz), 6.67 (1H, dd, J = 8.0, 2.0 Hz), 6.73 (1H, d, J = 8.0 Hz), 6.82 (1H, d, J = 8.0 Hz), 6.84 (1H, d, J = 2.0 Hz), 7.03 (1H, dd, J = 8.0, 2.0 Hz),7.13 (1H, t, br), 7.15 (1H, d, J = 2.0 Hz), 7.43 (1H, d, J = 15.5 Hz). HREIMS *m/z* 343.1417 (calcd for $C_{19}H_{21}NO_5$, 343.1420).

N-trans-feruloyl-4-methyldopamine (PA6): Colorless oil; yield 43%. IR (film) $_{max}$ 3400, 1600, 1510, 1210, 1200/cm. ^{1}H-NMR(acetone-d_6): δ2.72 (2H, t, J = 7.0 Hz), 3.49 (2H, q, J = 7.0 Hz), 3.80 (3H, s), 3.87 (3H, s), 6.49 (1H, d, J = 15.5 Hz), 6.65 (1H, dd, J = 8.0, 2.0 Hz), 6.73 (1H, d, J = 2.0 Hz), 6.82 (1H, d, J = 8.0 Hz), 6.84 (1H, d, J = 8.0 Hz), 7.03 (1H, dd, J = 8.0, 2.0 Hz), 7.15 (1H, d, J = 2.0 Hz), 7.16 (1H, t, br), 7.43 (1H, d, J = 15.5 Hz). HREIMS *m/z* 343.1417 (calcd for $C_{19}H_{21}NO_5$, 343.1420).

N-trans-isoferuloyl-dopamine (PA7): Yellow oil; yield 37%. IR (film) $_{max}$ 3400, 1650, 1510, 1270/cm. ^{1}H-NMR(acetone-d_6): δ2.69 (2H, t, J = 7.0 Hz), 3.48 (2H, q, J = 7.0 Hz), 3.85 (3H, s, -OCH_3), 6.49 (1H, d, J = 15.5 Hz), 6.55 (1H, dd, J = 8.0, 2.0 Hz), 6.73 (1H, d, J = 8.0 Hz), 6.72 (1H, d, J = 2.0 Hz), 6.92 (1H, d, J = 8.5 Hz), 6.98 (1H, dd, J = 8.5, 2.0 Hz), 7.06 (1H, d, J = 2.0 Hz), 7.34 (1H, t, -NH), 7.43 (1H, d, J = 15.5 Hz). HREIMS *m/z* 329.1284 (calcd for $C_{18}H_{19}NO_5$, 329.1263).

N-trans-isoferuloyl-3-methyldopamine (PA8): White solid; Mp 176-178℃; yield 62%. IR (KBr) $_{max}$ 3400, 1650, 1600, 1550, 1200/cm. ^{1}H-NMR(CD_3OD): δ2.76 (2H, t, *J* = 7.5 Hz), 3.47 (2H, t, *J* = 7.5 Hz), 3.82 (3H, s), 3.87 (3H, s), 6.38 (1H, d, *J* = 16.0 Hz), 6.66 (1H, dd, *J* = 8.0, 2.0 Hz), 6.71 (1H, d, *J* = 8.0 Hz), 6.81 (1H, d, *J* = 2.0 Hz), 6.91 (1H, d, *J* = 8.5 Hz), 6.98 (1H, dd, *J* = 8.5, 2.0 Hz), 7.02 (1H, d, *J* = 2.0 Hz), 7.40 (1H, d, *J* = 16.0 Hz). HREIMS *m/z* 343.1429 (calcd for $C_{19}H_{21}NO_5$, 343.1420).

N-trans-isoferuloyl-4-methyldopamine (PA9): White solid; Mp 163-165℃; yield 56%. IR (KBr) $_{max}$ 3300, 1650, 1515, 1250, 1200/cm. ^{1}H-NMR(acetone-d_6): δ2.72 (2H, t, *J* = 7.0 Hz), 3.49 (2H, q, *J* = 7.0 Hz), 3.80 (3H, s), 3.85 (3H, s), 6.47 (1H, d, *J* = 16.0 Hz), 6.65 (1H, dd, *J* = 8.5, 2.0 Hz), 6.83 (1H, d, *J* = 8.5 Hz), 6.93 (1H, d, *J* = 8.5 Hz), 6.99 (1H, dd, *J* = 8.5, 2.0 Hz), 7.03 (1H, d, *J* = 2.0 Hz), 7.22 (1H, t, -NH), 7.41 (1H, d, *J* = 16.0 Hz). ^{1}HREIMS *m/z* 343.1430 (calcd for $C_{19}H_{21}NO_5$, 343.1420).

N-trans-O-coumaroyl-3-methyldopamine (PA10): Colorless oil; yield 48%. IR (film) $_{max}$ 3400, 1655, 1600, 1510, 1250, 1200/cm. ^{1}H-NMR (acetone-d_6): δ2.78 (2H, t, *J* = 7.3 Hz), 3.54 (1H, m), 3.78 (3H, s, -OCH_3), 6.66 (1H, d, *J* = 8.0 Hz), 6.67 (1H, d, *J* = 8.0 Hz), 6.76 (1H, d, *J* = 8.0 Hz), 6.81 (1H, d, *J* = 16.0 Hz), 7.01 (1H, d, *J* = 8.0 Hz), 7.14 (1H, dd, *J* = 8.0, 2.0 Hz), 7.46 (1H, d, *J* = 8.0 Hz), 7.66 (1H, t, -NH), 7.93 (1H, d, *J* = 16.0 Hz). HREIMS *m/z* 313.1334 (calcd for $C_{18}H_{19}NO_4$, 313.1314).

N-trans-m-coumaroyl-3-methyldopamine (PA11): Colorless oil; yield 35%. IR (film) $_{max}$ 3400, 1655, 1610, 1510, 1250, 1200/cm. ^{1}H-NMR(acetone-d_6): δ2.76 (2H, t, *J* = 7.3 Hz), 3.52 (2H, m), 3.79 (3H, s, -OCH_3), 6.61 (1H, -NH), 6.65 (1H, d, *J* = 8.0 Hz), 6.66 (1H, d, *J* = 8.0 Hz), 6.74 (1H, d, *J* = 8.0 Hz), 6.85 (2H, m), 7.01 (2H, m), 7.19 (1H, d, *J* = 8.0 Hz), 7.48 (1H, d, *J* = 16.0 Hz). HREIMS *m/z* 313.1324 (calcd for $C_{18}H_{19}NO_4$, 313.1314).

N-trans-p-coumaroyl-3-methyldopamine (PA12): Colorless oil; yield 40%. IR

(film) $_{max}$ 3400, 1650, 1600, 1510, 1270, 1210/cm. ^{1}H-NMR(acetone-d_6): δ2.75 (2H, t, J = 7.2 Hz), 3.51 (2H, m), 3.80 (3H, s, -OCH_3), 6.49 (1H, d, J = 15.5 Hz), 6.64 (1H, d, J = 2.0 Hz), 6.69 (1H, dd, J = 8.0, 2.0 Hz), 6.76 (1H, d, J = 2.0 Hz), 6.82 (3H, m), 7.32 (1H, t, -NH), 7.41 (2H, m), 7.52 (1H, d, J = 15.5 Hz). HREIMS *m/z* 313.1332 (calcd for $C_{18}H_{19}NO_4$, 313.1314).

N-trans-O-coumaroyl-4-methyldopamine (PA13): Yellow oil; yield 30%. IR (film) $_{max}$ 3400, 1650, 1600, 1500, 1210/cm. ^{1}H-NMR(acetone-d_6): δ2.74 (2H, t, J = 7.3 Hz), 3.51 (2H, m), 3.79 (3H, s, -OCH_3), 6.66 (1H, dd, J = 8.0, 2.0 Hz), 6.73 (1H, d, J = 15.8 Hz), 6.75 (1H, d, J = 2.0 Hz), 6.82 (1H, d, J = 15.8 Hz), 6.83 (1H, d, J = 8.0 Hz), 6.95 (1H, dd, J = 8.0, 2.0 Hz), 7.17 (1H, m), 7.40 (1H, t, -NH), 7.46 (1H, dd, J = 8.0, 2.0 Hz), 7.89 (1H, d, J = 15.8 Hz). HREIMS *m/z* 313.1318 (calcd for $C_{18}H_{19}NO_4$, 313.1314).

N-trans-m-coumaroyl-4-methyldopamine (PA14): Colorless oil; yield 33%. IR (film) $_{max}$ 3400, 1650, 1610, 1500, 1250, 1210/cm. ^{1}H-NMR(acetone-d_6): δ2.73 (2H, t, J = 7.3 Hz), 3.50 (2H, m), 3.78 (3H, s, -OCH_3), 6.63 (1H, d, J = 2.0 Hz), 6.64 (1H, d, J = 15.7 Hz), 6.75 (1H, d, J = 2.0 Hz), 6.85 (1H, m), 7.00 (1H, d, J = 8.0 Hz), 7.04 (1H, d, J = 8.0 Hz), 7.19 (1H, t, J = 8.0 Hz), 7.43 (1H, d, J = 15.7 Hz). HREIMS *m/z* 313.1307 (calcd for $C_{18}H_{19}NO_4$, 313.1314).

N-trans-p-coumaroyl-3-methyldopamine (PA15): White solid; Mp 188-190℃; yield 40%. IR (film) $_{max}$ 3400, 1600, 1510, 1500, 1215/cm. ^{1}H-NMR(acetone-d_6): δ2.71 (2H, t, J= 7.3 Hz), 3.48 (2H, m), 3.79 (3H, s), 6.47 (1H, d, J = 15.7 Hz), 6.65 (1H, dd, J = 8.0, 2.0 Hz), 6.73 (1H, d, J = 2.0 Hz), 6.81 (1H, d, J = 2.0 Hz), 6.86 (1H, m), 7.28 (1H, -NH), 7.43 (1H, d, J = 8.0 Hz), 7.55 (1H, d, J =15.7 Hz) HREIMS *m/z* 313.1318 (calcd for $C_{18}H_{19}NO_4$, 313.1314).

2.4. In Vitro Assays

2.4.1. Assay of LDL Lipid Peroxidation

Blood samples were collected from healthy male adults after a 12 h overnight fasting. Sera were fractionated by ultracentrifugation (Beckman L8-80 M; R50 rotor) with the density adjusted by NaBr, LDL fractions ($1.019 < d < 1.063$ g/ml). To remove water-soluble antioxidants and NaBr, LDL (1.5 mg/mL) containing fractions (3-5 mL) were dialyzed extensively (at 4°C / N_2) against phosphate buffer saline (PBS, 50 mM; pH 7.4) in darkness. Dialyzed LDL was used for assay as soon as possible [12]. After dialysis, LDL was diluted with PBS to 0.9 mg cholesterol/mL. 50 μL aliquots of LDL in each well of a 96-well microtiter plate were incubated with $CuSO_4$ (final conc. 10 μM) at 37°C to induce lipid peroxidation. In a routine assay, incubation was carried out in the atmosphere at 37°C for 2 h (in a gyro-rotary incubator shaker at 120×g). For screening, LDL was pre-incubated with the test compounds at 37°C for 1 h before adding Cu^{2+}. After the test compounds were added, the mixture was incubated at 37°C for another 1 h. LDL oxidation was started by adding Cu^{2+}. Probucol (10 μM) was used as a positive control [13]. Routinely, the time course of conjugated diene formation was also determined by following the increase of the UV absorption at 232 nm. Prolongation of the lag phase was used present in LDL oxidation with Cu^{2+}. The lag phase and rate of oxidation of LDL are dependent on the contents of lipophilic antioxidants, particularly α-tocopherol and polyunsaturated fatty acids in LDL which may vary among individual donors.

2.4.2. Determination of DPPH Free Radical Scavenging Activity

Scavenging radical potency was evaluated using the DPPH test [14]. The different test compounds were dissolved in ethanol. DPPH in ethanol (40 mg/L, 750 μL) was

added to 750 μL of the test compounds at different concentrations in ethanol. Each mixture was then shaken vigorously and held for 30 min at room temperature and in the dark. The reaction mixture was taken in 96-well microtiter plates (Molecular Devices, USA). The decrease in absorbance of DPPH at 517 nm was measured. A blank is realized in the same conditions with 750 μL of ethanol. α-tocopherol were used as a positive control. All tests were performed in triplicate. Percent radical scavenging activity by compound treatment was determined by comparison with a deionized water-treated control group. IC_{50} values denote the concentration of compound which is required to scavenge 50% DPPH free radicals. The percentage of DPPH decolouration is calculated as follow: Inhibition DPPH (%) = 1 - (absorbance with compound/absorbance of the blank)×100. A plot of absorbance *vs* concentration was made to establish the standard curve and to calculate IC_{50} (Range from 0.001 to 0.000001M).

2.4.3. Determination of ORAC Assay

The ORAC assay as reported previously [15] with slight modifications. Briefly, the microplate equipped with an incubator and wavelength-adjustable fluorescence filters was used to monitor for the reaction. The temperature of the incubator was set at 37°C, and fluorescence filters with excitation wavelength of 480 nm and emission wavelength of 5250 nm were used. AAPH was used as peroxyl generator and Trolox was used as a antioxidant standard. Twenty microliters of suitablely diluted samples, blank, and Trolox calibration solutions were loaded to clear polystyrene 96-well microplates in triplicate based on a randomized layout. The plate reader was programmed to record the fluorescence of fluorescein one very cycle. Kinetic reading was recorded for 60 cycles with 40 s per cycle setting. Trolox standards were prepared

with PBS (75 mM, pH 7.0), which was used as blank. The samples were diluted with PBS (75 mM, pH 7.0) to the proper concentration range for fitting the linearity range of the standardcurve. After loading 20 μL of sample, standard and blank, and 200 μL of the fluorescein solution into appointed wells according to the layout, the microplate (sealed with film) was incubated for at least 30 min in the plate reader, then 20 μL of peroxyl generator AAPH (3.2 μM) was added to initiate the oxidation reaction. The final ORAC values were calculated using a linear equation between the Trolox standards or sample concentration and net area under the fluorescence decay curve. The data were analyzed using Microsoft Excel (Microsoft, Roselle, U.S.A.). The area under curve (AUC) was calculated as $AUC=0.5+(R_2/R_1+R_3/R_1+.....+0.5\ R_n/R_1)$, where R_1 was the fluorescence reading at the initiation of the reaction and R_n was the last measurement. The net AUC was obtained by subtracting the AUC of the blank from that of a sample or standard. The ORAC value was expressed as micro moles of Trolox equivalent per gram sample (μmole TE/g) using the calibration curve of Trolox. Linearity range of the calibration curve was 0 to 100 μM (r=0.99). For each specific sample, triplicate extractions were performed.

2.4.4. Evaluation of O_2^- Release by Polymorphonuclear Leukocytes (PMNs)

PMNs were isolated from the venous blood [16] of consenting healthy volunteers (20-35 years) by double-gradient Ficoll-Hypaque centrifugation and hypotonic lysis of contaminating red blood cells as previously described [17]. The cells were counted on a hemocytometer. PMN cells (1×10^6 cells/mL) pretreated with the various test agents (100 μM/L) at 37℃ for 5 min were stimulated with fMLP (1 μM) or PMA (0.16 μM) in the presence of lucigenin (0.48 mM). The reaction mixtures were then transferred to 96-well microplates and incubated at 37℃ for 15 min. Extracellular O_2^- production

was assessed with a luminometer. Chemiluminescence generated by PMA and fMLP alone respectively served as the reference controls. The percentage of superoxide inhibition of the test compound was calculated as the percentage of inhibition = {(control–resting)–(compound–resting)} ÷ (control–resting)×100.

2.4.5. Chemiluminescence with X / XO System

The reaction was carried out in a reaction mixture of 200 μL containing 120 μL of 50 mM Tris (pH 7.4), 48 μL of 2 mM lucigenin, and the various test compounds (100 μM). Subsequently, 8 μL of XO (0.02 U/ml) was added. The reaction was immediately started by the auto-injection of 24 μL of X (0.17 M). The superoxide-induced lucigenin chemiluminescence was measured using a luminometer (victor^3; Perkin Elemer). Activities of test compounds were calculated using the xanthine-inhibiting part of the chemiluminescence signal [18]. The results were expressed as percentages of inhibition enzyme activity.

2.5. In Vivo Assays

2.5.1. Animals

Male Sprague-Dawley rats, weighing 260-270 g, were purchased from the National Laboratory Animal Center. They were kept in an air-conditioned room (23±1 ℃, 50-60% humidity) light for 12 h/day (7 AM-7 PM). Our Institutional Animal Care and Use Committee approved the protocols for the animal study, and the animals were cared for in accordance with the institutional ethical guideline. After acclimatizing for 2 weeks with a commercial non-purified diet (rodent Laboratory Chow 5001, Purina Co., USA), 40 rats were divided into five groups of eight rats each. The diets were synthesized as described previously [19] and included: control diet, PA1 diet (1% PA1

in diet), PA1 diet (2% PA1), α-tocopherol diet (1% α-tocopherol) and α-tocopherol diet (2% α-tocopherol) for 8 weeks. On week 8, the rats were weighed and anesthetized with diethyl ether. Blood was obtained by heart puncture with syringes.

Plasma was collected by centrifugation (1,000 *g* × 15 *min*) from blood and analyzed using a Merck VITALAB Selectra Biochemical Autoanalyzer (Merck, Germany) to determine aspartate transferase (AST), alanine transferase (ALT) and alkaline phosphatase (ALP). Livers of the rats were quickly excised and weighed. Both relative ratios of liver weight to body weight were obtained. The liver was stored at -40ºC for glutathione peroxidase (GSH-Px) and thiobarbituric acid reactive substances (TBARS) determinations.

2.5.2. Antioxidant Activities

A 0.5 g sample of liver tissues were dissected, weighed, immersed in liquid N_2 for 60 s of death, and kept frozen at -70ºC. Prior to enzyme determinations, thawed tissue samples were homogenized on ice in 50 mM phosphate buffer (pH 7.4) and centrifuged at 3,200×3 *g* for 20 min at 5ºC. The supernatant was collected for antioxidant enzyme determinations.

(I) Determination of CAT activity

The liver homogenate was dissolved in 1.0 mL of a 0.25 M sucrose buffer. Ten microliters of the liver homogenate solution was added to a cuvette containing 2.89 mL of a 50 mM potassium phosphate buffer (pH 7.4), then the reaction was initiated by adding 0.1 mL of 30 mM H_2O_2 to make a final volume of 3.0 mL at 25°C. The decomposition rate of H_2O_2 was measured at 240 nm for 5 min to measure CAT activity. The activity was defined as the μmole/min/mg weight liver [20].

(Ⅱ) Determination of SOD activity

One hundred microliters of the cytosol supernatant was mixed with 1.5 mL of a Tris-EDTA-HCl buffer (pH 8.5) and 100 μL of 15 mM pyrogallol, and then incubated at 25°C for 10 min. The reaction was terminated by adding 50 μL of 1 N HCl and the absorbance at 440 nm. One unit was determined as the amount of enzyme that inhibited the oxidation of pyrogallol by 50%. Hepatic SOD activity was expressed as units/mg protein[21].

(Ⅲ) Determination of GSH-Px

Glutathione peroxidase (GSH-Px) levels were measured using the glutathione peroxidase assay kits (Calbiochem, Inc., San Diego, CA, USA). An equal volume of ice cold 10% metaphosphoric acid was added to the liver preparations. Supernatants were collected after centrifugation at 1000 rpm for 10 min and analyzed for GSH-Px as per manufacturer's instruction and expressed as unit/mg protein [22].

(Ⅳ) TBARS concentration

The liver tissue was homogenized, the subcellular fractions and thiobarbituric acid (TBA) and was incubated in boiling water for 30 min, centrifuged at 1,000×*g* for 25 min, and the supernatant was subsequently measured with a spectrophotometer (Hitachi, Japan) at 532 nm. TBARS concentration was expressed as nmolmalondialdehyde (MDA) g^{-1} liver or mL^{-1} serum [23].

2.5.3. Determination Total Protein

Protein content in each sample was determined by a bicinchoninic acid (BCA) protein

assay kit (Pierce).

(I) Determination of serum TNF-α and NF-κB level by ELISA

Serum levels of TNF-α and NF-κB were determined using a commercially available enzyme linked immunosorbent assay (ELISA) kit (Biosource International Inc., Camarillo, CA) according to the manufacturer's instruction. TNF-α and NF-κB by using a standard curve. The concentrations were both expressed by pg/mg protein.

(II) Determination of nitric oxide/nitrite level

NO concentrations was indirectly assessed by measuring the nitrite levels in serum determined by a calorimetric method based on the Griess reaction. Serum samples were diluted four times with distilled water and deproteinized by adding 1/20 volume of zinc sulphate (300 g/L) to a final concentration of 15 g/L. After centrifugation at 10,000 g for 5 min at room temperature, 100 µl supernatant was applied to a microtiter plate well, followed by 100 µl of Griess reagent (1% sulphanilamide and 0.1% N-1-naphthylethylenediamine dihydrochloride in 2.5% polyphosphoric acid). After 10 min of colour development at room temperature, the absorbance was determined at 540 nm with a Micro-Reader (Molecular Devices, Orleans Drive, Sunnyvale, CA). By using sodium nitrite to generate a standard curve, the concentration of nitrite was determined at 540 nm.

2.6. Statistical Analysis

All values in the text and figures are given as means±S.E.M. Data are analyzed by one-way analyses of variance (ANOVA) depending on the number of experimental variables followed by post-hoc Dunnett's *t*-test for multiple comparisons.

Concentration dependence was analyzed by simple linear regression analysis of response levels against concentrations of compounds and testing the slope of the regression line against 0 by Student's *t*-test. Values of human neutrophils $p<0.05$ were considered significant.

3. Results and discussion

3.1. In Vitro Evaluations

3.1.1. Inhibition of LDL Oxidation Activity

An elevated concentration of plasma LDL is a major risk factor for atherosclerosis. LDL oxidation can be studied in vitro by following the generation of oxidation products during Cu^{2+} catalysed oxidation [24]. The in vitro oxidation may reflect in vivo oxidation as the resistance of LDL towards in vitro oxidation has been found to be correlated with the extent of coronary atherosclerosis [25]. Antioxidant activity was based on the inhibition of conjugated diene formation. It has been documented that Cu^{2+} induced Ox-LDL exhibits biological and immunological properties similar to those *in vivo*. Cu^{2+}-induced Ox-LDL is recognizable by scavenger receptors and causes cholesterol ester accumulation in macrophages [26]. In screening for antioxidants to inhibit LDL oxidation, this method is simple and commonly used. Antioxidants able to inhibit LDL oxidation may reduce early atherogenesis and slow down the progression to advance stages. Control antioxidant of probucol is a lipid-lowering drug can inhibit LDL oxidation and reduce atherosclerosis in experimental animals which was used as a reference antioxidant on inhibition of LDL oxidation [27].

The IC_{50} value of PA1-PA15 in the inhibition of Cu^{2+}-induced LDL lipid

oxidation is shown in Table 2. Compounds PA 1, PA 3, PA 5, PA 7, PA 9 and PA 10 showed higher activities on inhibition of Cu^{2+}-induced LDL oxidation than control antioxidant of probucol. When phenolics function as antioxidants direct radical scavenging mechanisms, they are univalently oxidized to their respective phenoxyl radicals [28]. However, until recently, these radicals had been difficult to detect by static electron spin resonance (ESR) because they rapidly change to non-radical products.

3.1.2. Effect of DPPH and ORAC Activity

DPPH is one of the strategies used to evaluate the antioxidant properties of plant extracts; this method has shown to be rapid and simple and it measures the capacity of plant extract to the DPPH radical, a nitrogen-centred free radical [29]. The structural changes that this radical provokes on plant principles as well as the involved mechanism are not clear yet [30].

Oxidative stress represents an imbalance between the production and manifestation of reactive oxygen species and a biological system's ability to readily detoxify the reactive intermediates or to repair the resulting damage. Disturbances in the normal redox state of tissues can cause toxic effects through the production of peroxides and free radicals that damage all components of the cell, including proteins, lipids, and DNA. Some reactive oxidative species can even act as messengers through a phenomenon called redox signaling.

The effect of the PAs derivatives scavenging activity of phenolic acids on the DPPH radicals was investigated. For performing the DPPH assay, a solution of the purple coloured DPPH radical was mixed with the test compound and the decrease of the absorption was determined photometrically until a steady state was reached. The concentration of phenolic acids and DPPH ethanolic solutions were 1.0×10^{-4} (Table 3).

455 The ORAC assay has been used to study the antioxidant capacity of many compounds
456 and food samples [15]. ORAC antioxidant capacity of PAs ranged from 21.57 μmole
457 TE/g to 49.23 μmole TE/g, the values obtained are shown in Table 3.

458 These compounds also possess a direct scavenger effect on trapping DPPH
459 radicals. α-tocopherol (the lipid soluble vitamin E analogue) was used as a positive
460 control in the study. We also found that PAs (compounds PA1, PA2, PA3, PA5 and
461 PA7) were better than α-tocopherol. The results are presented PA1 was the most
462 potent compound, nearly 3.5 times as α-tocopherol, compounds PA2, PA3 and PA7
463 also reduced DPPH radicals are efficient radical scavengers and antioxidants and
464 more effective as radical scavengers when compared with the standards α-tocopherol
465 than compounds PA4 and PA11 (Fig. 1). The investigated amides are equal or more
466 potent antioxidants for soybean and evening primrose oil with respect to α-tocopherol.
467 They are able to protect squalene against oxidation fairly well, but are inferior to
468 classic antioxidants like α-tocopherol. From these we obtained that the radical
469 scavenging activity increased with increasing numbers of hydroxy groups on catechol
470 moiety in this series of phenolic amides.

471 Catechol is a polyhydroxy organic compound, which is widely used in industry.
472 It is able to form adjacent hydrogen bonds with proton acceptors that can significantly
473 affect its reactivity and antioxidant capacity. The UV light had a synergistic effect on
474 decomposing H_2O_2 to produce reactive species for catechol oxidation. In catechol
475 oxidation under initial pH of 7.0, formic acid, acetic acid, oxalic acid, and maleic acid
476 were produced and caused solution pH decrease to acidic condition favorable for high
477 oxidation performance [31, 32].

478

479 *3.1.3 Evaluation of Superoxide Anions Release by Human Neutrophils and Scavenger*

480 *of Superoxide Radicals in X/XO System*

481

482 The effect of the PAs derivatives on superoxide generation in human neutrophils
483 was investigated. Superoxide anion production was induced by PMA or fMLP,
484 respectively and detected by lucigenin chemiluminescence. Neutrophilic superoxide
485 generation has been linked to various types of inflammation. The superoxide
486 generation in human neutrophils is stimulated during phagocytosis or exposure to
487 various stimuli [33]. Superoxide anion production induced by PMA or fMLP with
488 different mechanisms and detected by lucigenin chemiluminescence is carried in this
489 study [34].

490 In our recently results, we found phenolic acids and their ester derivatives
491 display potent anti-inflammatory activity against PMA and fMLP-induced superoxide
492 anion production [35]. Here we also determined the activity of PAs in human neutrophil
493 superoxide anion production. The inhibitory effect on the PMA-induced superoxide
494 generation by PAs was PA8 (35.4%) > PA12 (33.9□%) > PA10 (25%) and the
495 fMLP-induced was PA2 (74.3%) > PA9 (70.1%) > PA8 (55.3%) (Table 4).
496 Compounds PA3, PA5 and PA9 gave no effect and others showed only slight effect
497 on PMA-induced response. Most of these phenolic amides were able to affect the
498 fMLP-induced superoxide generation. Therefore, we assumed these PAs inhibited
499 preferentially fMLP-induced superoxide generation indicated a calcium-dependent
500 signaling pathway rather than a PKC-dependent mechanism.

501 Superoxide is generated in vivo by several mechanisms including the activation
502 of neutrophils and by the action of X/XO, XO enzyme is a physiological source of
503 superoxide anions in eukaryotic cells.

504 Using the X/XO system, the superoxide scavenging capacity was evaluated by

chemiluminescence. In early study, we found phenolic acids slightly inhibited superoxide in X/XO system. Compounds PA1 (41.6%), PA4 (36.2%) and PA5 (36.7%) showed efficient inhibitory action on scavenging superoxide production by the X/XO system, but PA7, PA8, PA10 and PA11 did not show direct quenching effect on the lucigenin signals (Table 4).

3.2. Effect of Antioxidative and Anti-inflammatory in Rats

The hepatic antioxidant enzyme activities of SOD and CAT were increased in the liver of rats treated with PA1 and α-tocopherol treated model group, however, the activities of SOD and CAT of PA1 (2%) group were better than PA1 (1%), α-tocopherol (1%) and α-tocopherol (2%) groups. As shown in Table 5, the hepatic GSH-Px level was significantly (p<0.05) increased by PA1 (2%) treatment group when compared with the PA1 (1%), α-tocopherol (1%) and α-tocopherol (2%) groups.

SOD, CAT and GSH-Px play the roles to eliminate these free radicals in i*n vivo*. A great deal of research indicated that when organism suffered from oxidative damage, its antioxidative mechanism would be activated because of the oxidation pressure, causing considerable expression of antioxidant enzymes.

Effect of anti-inflammatory of PA1 and α-tocopherol on the serum levels of TNF-α, NF-κB and NO in rats. As shown in Table 5, the PA1 and α-tocopherol treatment group caused a significant (p<0.05) decreased in the level of TNF-α/NF-κB in the serum when compared with the control group. Mice treated with PA1 (2%) also showed a significant (p<0.05) decrease of NO production in serum compared with the PA1 (1%), α-tocopherol (1%) and α-tocopherol (2%) groups, the production of NO in model group serum was significantly decreased in the PA1 and α-tocopherol treated

model group compared to the control group.

Pro-inflammatory cytokine (TNF-α and NO), is rapidly produced by macrophages in response to tissue damage. Whereas low levels of TNF-α may play a role in cell protection, excessive amounts cause cell impairment. TNF-α also stimulates the release of cytokines from macrophages and induces the phagocyte oxidative metabolism and nitric oxide production [36]. Activated macrophages result in increases of NF-κB-dependent inflammatory mediators [37]. NF-κB activation and the other inflammatory factors are well-known biological markers for inflammatory responses.

In conclusion, we prepared a series of 15 PAs and demonstrated that PA5 and PA9 were better inhibitors of LDL oxidation but PA1 was the most potent compound on scavenging DPPH, the superoxide generation induced by fMLP (1.0 μM) and PMA (0.16 μM) was inhibited to various degrees with compounds PA8 and PA12 significantly, in human neutrophils and scavenging superoxide by X/XO system as detected by lucigenin chemiluminescence is worth to note that PA1, PA2, PA4 and PA5 more efficient inhibitory action on XO activity. Our results clearly showed that PAs exhibited antioxidative activity. The substitution of a hydroxy or methoxy group for R_1-R_5 function group led to PAs compounds endowed with very high antioxidant activity. Fortification of diets with food materials rich in PAs has been shown to impart antimutagenic, anti-inflammatory and antioxidant properties, which can be exploited in developing health foods or cosmetics [38]. PAs derivatives, such as caffeic acid phenethyl ester (CAPE, 1) from the propolis of honeybee hives, have been investigated in recent years [39]. It has been shown that CAPE displays oxidation, lipooxygenase and protein tyrosine kinase inhibition, as well as NF-κB activation properties [40]. PAs may let us in developing drugs may exert their anti-inflammatory

action through inhibiting superoxide generation which can help aging problems such as Parkinson's disease, dementia, etc, caused by oxidative stress.

In humans, oxidative stress is involved in many diseases. Examples include Sickle cell disease [41], atherosclerosis, Parkinson's disease, heart failure, myocardial infarction, Alzheimer's disease, Schizophrenia, Bipolar disorder, fragile X syndrome [42] and chronic fatigue syndrome, but short-term oxidative stress may also be important in prevention of aging by induction of a process named mitohormesis [43]. Reactive oxygen species can be beneficial, as they are used by the immune system as a way to attack and kill pathogens.

Acknowledgements

This study was supported by Ministry of Science and Technology (MOST 103-2622-B-040-001-CC3, MOST 104-2320-B-040-018).

References

1. D. Sumczynski, Z. Bubelova, J. Sneyd, S. Erb-Weber and J. Mlcek, Total phenolics, flavonoids, antioxidant activity, crude fibre and digestibility in non-traditional wheat flakes and muesli. *Food Chem.,* 2015, 174, 319–325.
2. H. J. Forman, K. J.A. Davies and F. Ursini, How do nutritional antioxidants really work: Nucleophilic tone and para-hormesis versus free radical scavenging *in vivo*. *Free Rad. Biol. Med.,* 2014, 66, 24–35.
3. N. Hamada and Y. Fujimichi, Role of carcinogenesis related mechanisms in cataractogenesis and its implications for ionizing radiation cataractogenesis. *Cancer Lett.,* 2015, *In Press*.
4. L. Zuo and M. S. Motherwell, The impact of reactive oxygen species and genetic mitochondrial mutations in Parkinson's disease. *Gene*, 2013, 532, 18–23.
5. Y. F. Bao, J. Y. Li, L. F. Zheng and H. Y. Li, Antioxidant activities of cold-nature Tibetan herbs are signifcantly greater than hot-nature ones and are associated with their levels of total phenolic components. *Chin. J. Nat. Med.,* 2015, 13, 609–617.
6. N. Harris, F. Y. Kogan, G. Il'kova, S. Juhas, O. Lahmy, Y. I. Gregor, J. Koppel, R. Zhuk and P. Gregor, Small molecule inhibitors of protein interaction with glycosaminoglycans (SMIGs), a novel class of bioactive agents with anti-inflammatory properties. *Bioch. Biophys. Acta,* 2014, 1840, 245–254.
7. Y. Zhong, Y. S. Chiou, M. H. Pan, C. T. Ho and F. Shahidi, Protective effects of epigallocatechin gallate (EGCG) derivatives on azoxymethane-induced colonic carcinogenesis in mice. *J. Funct. Foods*, 2012, 4, 323–330.
8. Y. Zhong, C. M. Ma and F. Shahidi, Antioxidant and antiviral activities of lipophilic epigallocatechin gallate (EGCG) derivatives. *J. Funct. Foods*, 2012, 4, 87–93.

9. S. Sen, R. Chakraborty and B. De, Challenges and opportunities in the advancement of herbal medicine: India's position and role in a global context. *J. Herbal Med.,* 2011, 1, 67–75.

10. L. Yang, H. Jiang, Q. H. Wang, B. Y. Yang and H. X. Kuang, A new feruloyl tyramine glycoside from the roots of Achyranthes bidentata. *Chin. J. Nat. Med.,* 2012, 10, 16-19.

11. I. Celik, A. Temur and I. Isik, Hepatoprotective role and antioxidant capacity of pomegranate (*Punica granatum*) flowers infusion against trichloroacetic acid exposed in rats. *Food Chem. Toxicol.*, 2009, 47, 145–149.

12. H. Katouah, A. Chen, I. Othman and S. P. Gieseg, Oxidised low density lipoprotein causes human macrophage cell death through oxidant generation and inhibition of key catabolic enzymes. *Int. J. Biochem. Cell Biol.,* 2015, 67, 34–42.

13. C. X. Liu, R. Liu, H. R. Fan, X. F. Xiao, X. P. Chen, H. Y. Xu and Y. P. Lin, Network pharmacology bridges traditional application and modern development of traditional chinese medicine. *Chin. Herbal Med.,* 2015, 7, 3–17.

14. E. S. Hwang and G. H. Kim, Biomarkers for oxidative stress status of DNA, lipids, and proteins *in vitro* and *in vivo* cancer research. *Toxicology*, 2007, 229, 1–10.

15. B. J. Xu, S. H. Yuan and S. K. C. Chang, Comparative analyses of phenolic composition and antioxidant capacity of cool season legumes with other selected food legumes. *J. Food Sci.,* 2007, 72, S167–S177.

16. O. Sulaieva, V. Deliy and S. Zharikov, Relationship between leukocytes recruitment and risk of rebleeding in patients with peptic ulcers. *Pathophysiology,* 2015, *In Press*.

17. M. Vazzana, M. Celi, C. Tramati, V. Ferrantelli, V. Arizza and N. Parrinello, In vitro effect of cadmium and copper on separated blood leukocytes of

Dicentrarchus labrax. *Ecotoxicol. Environ. Saf.,* 2014, 102, 113–120.

18. J. E. Benna, P. M. C. Dang and M. B. Yaffe, The phagocyte NADPH oxidase: structure and assembly of the key multicomponent enzyme of innate immunity. *Encycl. Cell Biol.,* 2016, 3, 702–709.

19. Y. L. Hsieh, Y. H. Yeh, Y. T. Lee and C. Y. Huang, Protective effects of Cholestin on ethanol induced oxidative stress in rats. *J. Sci. Food Agric.,* 2015; 95, 799–808.

20. K. Liu, Y. Zhao, F. Chen and Y. Fang, Purification and identification of Se-containing antioxidative peptides fromenzymatic hydrolysates of Se-enriched brown rice protein. *Food Chem.,* 2015, 187, 424–430.

21. J. Yu, L. Ge, S. Liu, P. Dai, S. Ge and W. Zheng, Facile and scalable synthesis of ba novel rigid artificial superoxide dismutasebased on modified hollow mesoporous silica microspheres. *Biosens. Bioelectr.,* 2011, 26, 1936–1941.

22. D. Peng, A. Belkhiri and W. El-Rifai, Regulation of oxidative DNA damage by glutathione peroxidase 7 in Barrett's tumorigenesis. *Gastroenterol.,* 2011, 140, S-104.

23. B. Kong, X. Peng, Y. L. Xiong and X. Zhao, Protection of lung fibroblast MRC-5 cells against hydrogen peroxide-induced oxidative damage by 0.1–2.8 kDa antioxidative peptides isolated from whey protein hydrolysate. *Food Chem.,* 2012, 135, 540–547.

24. D. de Gonzalo-Calvo, A. Cenarro, M. Martínez-Bujidos, L. Badimon, A. Bayes-Genis, J. Ordonez-Llanos, F. Civeira and V. Llorente-Cortés, Circulating soluble low-density lipoprotein receptor-related protein 1 (sLRP1) concentration is associated with hypercholesterolemia: A new potential biomarker for atherosclerosis. *Int. J. Cardiol.,* 2015, 201, 20–29.

655 25. K. Nakajima, T. Nakano and A. Tanaka, The oxidative modification hypothesis of
656 atherosclerosis: the comparison of atherogenic effects on oxidized LDL and
657 remnant lipoproteins in plasma. *Clin. Chim. Acta*, 2006, 367, 36–47.
658 26. M. Rosenblat, N. Volkova, R. Coleman, Y. Almagor and M. Aviram,
659 Antiatherogenicity of extra virgin olive oil and its enrichment with green tea
660 polyphenols in the atherosclerotic apolipoprotein-E-deficient mice: enhanced
661 macrophage cholesterol efflux. *J. Nutr. Biochem.,* 2008, 19, 514–523.
662 27. F. Otsuka, M. C. A. Kramer, P. Woudstra, K. Yahagi, E. Ladich, Aloke V. Finn,
663 Robbert J. de Winter, Frank D. Kolodgie, Thomas N. Wight, Harry R. Davis, M.
664 Joner and R. Virmani, Natural progression of atherosclerosis from pathologic
665 intimal thickening to late fibroatheroma in human coronary arteries: A pathology
666 study. *Atherosclerosis,* 2015, 241, 772–782.
667 28. F. M. F. Roleira, E. J. Tavares-da-Silva, C. L. Varela, S. C. Costa, T. Silva, J.
668 Garrido, and F. Borges, Plant derived and dietary phenolic antioxidants:
669 Anticancer properties. *Food Chem.,* 2015, 183, 235–258.
670 29. M. E. Letelier, A. Molina-Berríos, J. Cortés-Troncoso, J. Jara-Sandoval, M. Holst,
671 K. Palma, M. Montoya, D. Miranda and V. González-Lira, DPPH and oxygen
672 free radicals as pro-oxidant of biomolecules. *Toxicol In Vitro* 2008, 22, 279–286.
673 30. Y. Zhang, Y. Shen, Y. Zhu and Z. Xu, Assessment of the correlations between
674 reducing power, scavenging DPPH activity and anti-lipid-oxidation capability of
675 phenolic antioxidants. *LWT-Food Sci. Technol.,* 2015, 63, 569–574.
676 31. M. A. Varfolomeev, A. E. Klimovitskii, D. I. Abaidullina, T. I. Madzhidov and B.
677 N. Solomonov, “Additive” cooperativity of hydrogen bonds in complexes of
678 catechol with proton acceptors in the gas phase: FTIR spectroscopy and quantum
679 chemical calculations. *Spectrochim. Acta A Mol. Biomol. Spectrosc.*, 2014, 91,

75–82

32. W. Li, Y. Wang and A. Irini, Effect of pH and H_2O_2 dosage on catechol oxidation in nano-Fe_3O_4 catalyzing UV–Fenton and identification of reactive oxygen species, *Chem. Eng. J.,* 2014, 244, 1–8

33. B. Friedrichs, U. Neumann, J. Schüller and M. J. Peck, Cigarette-smoke-induced priming of neutrophils from smokers and non-smokers for increased oxidative burst response is mediated by TNF-α. *Toxicol. In Vitro*, 2014, 28, 1249–1258.

34. X. Ren, F. Lv, B. Fang, S. Liu, H. Lv, G. He, H. Ma, Y. Cao and Y. Wang, Anesthetic agent propofol inhibits myeloid differentiation factor 88-dependent and independent signaling and mitigates lipopolysaccharide-mediated reactive oxygenspecies production in human neutrophils *in vitro*. *Eur. J. Pharm.*, 2014, 744, 164–172.

35. Y. T. Lee, M. J. Don, C. H. Liao, H. W. Chiou, C. F. Chen and L. K. Ho, Effects of phenolic acid esters and amides on stimulus-induced reactive oxygen species production in human neutrophils. *Clin. Chim. Acta,* 2005, 352, 135–141.

36. T. Leibovich-Rivkin, Y. Liubomirski, B. Bernstein, T. Meshel and A. Ben-Baruch, Inflammatory factors of the tumor microenvironment induce plasticity in nontransformed breast epithelial cells: EMT, invasion, and collapse of normally organized breast textures. *Neoplasia,* 2013, 15, 1330–1346.

37. P. Di Tomo, R. Canali, D. Ciavardelli, S. Di Silvestre, A. De Marco, A. Giardinelli, C. Pipino, N. Di Pietro, F. Virgili and A. Pandolfi, β-Carotene and lycopene affect endothelial response to TNF-α reducing nitro-oxidative stress and interaction with monocytes. *Mol. Nutr. Food Res.*, 2012, 56, 217–227.

38. D. Kalita, D. G. Holm and S. S. Jayanty, Role of polyphenols in acrylamide formation in the fried products of potato tubers with colored flesh. *Food Res. Int.,*

2013, 54, 753–759.

39. K. Wang, J. Zhang, S. Ping, Q. Ma, X. Chen, H. Xuan, J. Shi, C. Zhang and F. Hu, Anti-inflammatory effects of ethanol extracts of Chinese propolis and buds from poplar (*Populus canadensis*). *J. Ethnopharmacol.,* 2014, 155, 300–311.

40. J. Hyeog Choi, K. H. Roh, H. Oh, S. J. Park, S. M. Ha, M. S. Kang, J. H. Lee, S. Y. Jung, H. Song, J. W. Yang and S. G. Park, Caffeic acid phenethyl ester lessens disease symptoms in an experimental autoimmune uveoretinitis mouse model. *Exp. Eye Res.,* 2015, 134, 53–62.

41. J. Amer, H. Ghoti, E. Rachmilewitz, A. Koren, C. Levin and E. Fibach, Red blood cells, platelets and polymorphonuclear neutrophils of patients with sickle cell disease exhibit oxidative stress that can be ameliorated by antioxidants. *Brit. J Haematol.,* 2006, 132, 108-113

42. Y. De Diego-Otero, Y. Romero-Zerbo, R. el Bekay, J. Decara, L. Sanchez, F. Rodriguez-de Fonseca and I. del Arco-Herrera Alpha-tocopherol protects against oxidative stress in the fragile X knockout mouse: an experimental therapeutic approach for the Fmr1 deficiency. *Neuropsychopharmacology,* 2009, 34, 1011–1026.

43. D. Gems and L. Partridge, Stress-response hormesis and aging: that which does not kill us makes us stronger. *Cell Metab.,* 2008, 7, 200–203.

731 Table 1. Structure of phenolic amides (PA1-PA15)

Compound	R_1	R_2	R_3	R_4	R_5
PA1	OH	H	H	OH	OH
PA2	H	OH	H	OH	OH
PA3	H	H	OH	OH	OH
PA4	H	OMe	OH	OH	OH
PA5	H	OH	OMe	OH	OH
PA6	OH	H	H	OMe	OH
PA7	H	OH	H	OMe	OH
PA8	H	H	OH	OMe	OH
PA9	H	OMe	OH	OMe	OH
PA10	H	OH	OMe	OMe	OH
PA11	OH	H	H	OH	OMe
PA12	H	OH	H	OH	OMe
PA13	H	H	OH	OH	OMe
PA14	H	OMe	OH	OH	OMe
PA15	H	OH	OMe	OH	OMe

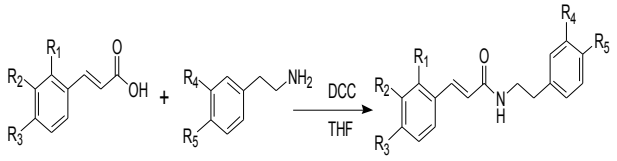

1, R_1= OH, R_2= R_3= H
2, R_1= R_3= H, R_2= OH
3, R_1= R_2= H, R_3= OH
4, R_1= H, R_2= OMe, R_3= OH
5, R_1= H, R_2= OH, R_3= OMe

a, R_4= R_5= OH
b, R_4= OMe, R_5= OH
c, R_4= OH, R_5= OMe

PA1-PA15

732

733

734

735

736

Table 2. The IC_{50} value[a] of phenolic amides (PA1-PA15) in the inhibition of Cu^{2+}-induced LDL lipid oxidation

Compound	LDL oxidation IC_{50} (μM)[a]	Rel. potency to probucol[c]
PA1	3.2 ± 0.3	1.3 ± 0.2
PA2	3.7 ± 0.2	1.0 ± 0.1
PA3	5.0 ± 0.8	1.1 ± 0.1
PA4	3.6 ± 0.1	0.8 ± 0.1
PA5	3.3 ± 0.4	1.4 ± 0.0
PA6	7.1 ± 0.5	0.5 ± 0.3
PA7	4.0 ± 0.7	1.2 ± 0.1
PA8	9.9 ± 1.0	0.4 ± 0.2
PA9	2.9 ± 0.1	1.4 ± 0.2
PA10	3.1 ± 0.4	1.3 ± 0.1
PA11	5.9 ± 1.1	1.0 ± 0.1
PA12	5.8 ± 1.2	0.4 ± 0.1
PA13	4.1 ± 0.6	0.7 ± 0.1
PA14	3.0 ± 0.3	0.7 ± 0.1
PA15	2.8 ± 0.3	1.0 ± 0.1
Probucol[b]	3.9 ± 0.2	1.0

[a] Results of inhibition LDL oxidation were expressed as mean± S.E.M. from three experiments with duplicated determination, where human blood samples were taken as the test sources. Each IC_{50} value indicated the concentration of compounds required to inhibit the formation of conjugated diene in Cu^{2+}-induced LDL oxidation by 50%.

[b]Probucol was used as a positive control drug.

[c]The relative potency of each compound was expressed as IC_{50} (Probucol) / IC_{50} (Compound). For a compound exhibiting equal relative potency value was set as 1.0. Since the IC_{50} values are LDL dependent, the IC_{50} of probucol in the same LDL preparation used for assay was also enclosed.

Table 3. Scavenging activity of antioxidants for DPPH radical[a] and ORAC; data are shown as IC_{50} (μM)[b] and percentage inhibition at 0.1M of antioxidants[c]

Compound[e]	Inhibition,% (±S.E.M.)	IC_{50} (M)	Relative potency[d]	Antioxidant capacity (μmole TE/g)
α-tocopherol	51.0 ± 0.1	9.68×10^{-5}	1.0	32.56±1.16
PA1	78.3 ± 0.1	2.78×10^{-5}	3.48	49.23±2.26
PA2	73.8 ± 0.1	3.64×10^{-5}	2.66	41.52±0.32
PA3	72.8 ± 0.1	4.54×10^{-5}	2.13	42.21±0.15
PA4	24.1 ± 0.3	4.06×10^{-4}	0.24	23.21±0.23
PA5	63.9 ± 0.1	6.98×10^{-5}	1.39	35.78±1.16
PA6	42.7 ± 0.1	1.65×10^{-4}	0.59	26.62±0.21
PA7	76.0 ± 0.5	3.45×10^{-5}	2.81	45.58±0.23
PA8	45.4 ± 0.2	1.55×10^{-4}	0.63	22.32±0.23
PA9	33.5 ± 0.4	2.88×10^{-4}	0.34	23.52±1.26
PA10	38.9 ± 0.4	2.17×10^{-4}	0.45	27.63±0.21
PA11	31.5 ± 1.1	8.74×10^{-4}	0.11	26.23±0.15
PA12	33.7 ± 0.6	2.79×10^{-4}	0.35	22.32±0.13
PA13	28.4 ± 1.2	3.48×10^{-4}	0.28	21.57±0.20
PA14	33.8 ± 0.3	2.79×10^{-4}	0.35	25.65±1.13
PA15	38.0 ± 0.3	2.25×10^{-4}	0.43	23.78±0.22

[a] The final concentration of DPPH ethanolic solution was 1.0×10^{-4} M.
[b] The IC_{50} (M) values were calculated from the slope equations of the dose-response curves.
[C] Values are expressed as mean ± S.E.M. from three independent experiments. Values with different superscripts are significant difference ($p<0.05$).
[d] The relative potency of each compound was expressed as IC_{50} (α-tocopherol) / IC_{50} (compound). α-tocopherol, relative potency value was set as 1.0.

Table 4. Inhibition (%) of phenolic amides (PA1-PA15) on PMA- or fMLP-induced superoxide generation in human neutrophils and scavenging superoxide by xanthine/xanthine oxidase system

Compound	PMA	fMLP	xanthine/xanthine oxidase
PA1	15.2 ± 4.9	52.4 ± 14.1	41.6 ± 1.7
PA2	16.2 ± 7.1	74.3 ± 10.6	27.6 ± 1.3
PA3	No effect	43.0 ± 8.6	14.4 ± 7.2
PA4	8.3 ± 4.1	13.9 ± 7.2	36.2 ± 1.9
PA5	No effect	9.2 ± 5.2	36.7 ± 2.5
PA6	15.7 ± 4.5	33.1 ± 1.3	8.5 ± 2.6
PA7	11.3 ± 6.3	23.7 ± 8.9	No effect
PA8	35.4 ± 7.4	55.3 ± 3.4	No effect
PA9	No effect	70.1 ± 1.1	2.3 ± 0.2
PA10	25.0 ± 2.2	47.7 ± 13.0	No effect
PA11	15.8 ± 7.8	48.2 ± 3.9	No effect
PA12	33.9 ± 8.2	50.7 ± 2.2	2.0 ± 0.5
PA13	8.9 ± 3.9	32.5 ± 3.6	9.7 ± 0.1
PA14	7.7 ± 2.1	14.8 ± 1.3	6.0 ± 0.5
PA15	21.9 ± 1.9	17.2 ± 5.0	17.9 ± 0.9

The cells were preincubated with 100 μmmol/l of compounds for 5 min prior to the addition of PMA (0.16 μmmol/l) or fMLP (1.0 μmmol/l). Results are expressed as mean ± S.E.M. from six independent experiments.

Table 5. Effect of PA1 and α-tocopherol on SOD, CAT, GPx, GR, TNF-α, NF-κB and NO levels in SD rats

Levels	Control [x]	PA1 (1%)[y]	PA1 (2%)	α-Tocopherol (1%)	α-Tocopherol (2%)
SOD (unit/mg weight liver)	1.15±0.08[a]	1.69±0.05[b]	1.83±0.06[c]	1.46±0.07[b]	1.57±0.06[b]
CAT (μmole/min/mg weight liver)	125±11[a]	157±16[b]	188±15[c]	146±13[b]	153±15[b]
GSH-Px (μM/g weight liver)	36.5±6.7[a]	65.5±55.2[b]	89.5±7.2[c]	68.5±5.6[b]	73.6±6.5[b]
TBARS (nM/ml weight liver)	0.027±0.001[a]	0.022±0.02[b]	0.018±0.001[c]	0.022±0.001[b]	0.021±0.002[b]
TBARS (nM/ml weight plasma)	1.92±0.06[a]	1.58±0.05[b]	1.23±0.03[c]	1.52±0.05[b]	1.47±0.06[b]
TNF-α (pg/ml)	88±2[c]	77±6[b]	66±5[a]	75±3[b]	69±7[b]
NF-κB (pg/ml)	95±5[c]	76±2[b]	69±3[a]	73±6[b]	61±2[b]
NO (μm)	5.3±0.1[b]	4.6±0.2[a]	4.3±0.3[a]	4.3±0.5[a]	4.2±0.3[a]

SOD: superoxide dismutase, CAT: catalase, GSH-Px: glutathione peroxidase, TBARS: thiobarbituric acid reactive substances, TNF-α: tumor necrosis factor-alpha, NF-κB: nuclear factor-kappa B, NO: nitric oxide.

[x] Different letters (a−c) are significantly different between the control and treated groups (p<0.05), Mean ± SD (N = 8).

[y] 1% at doses of 16.67 mg/kg, 2% at doses of 33.34 mg/kg.

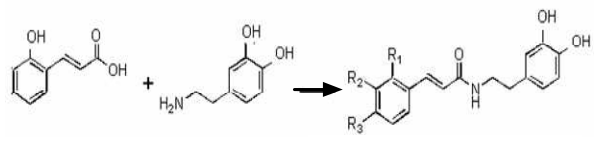

2-hydroxycinnamic acid 3-hydroxytyramine *N-trans-O*-coumaroyldopamine (PA1)

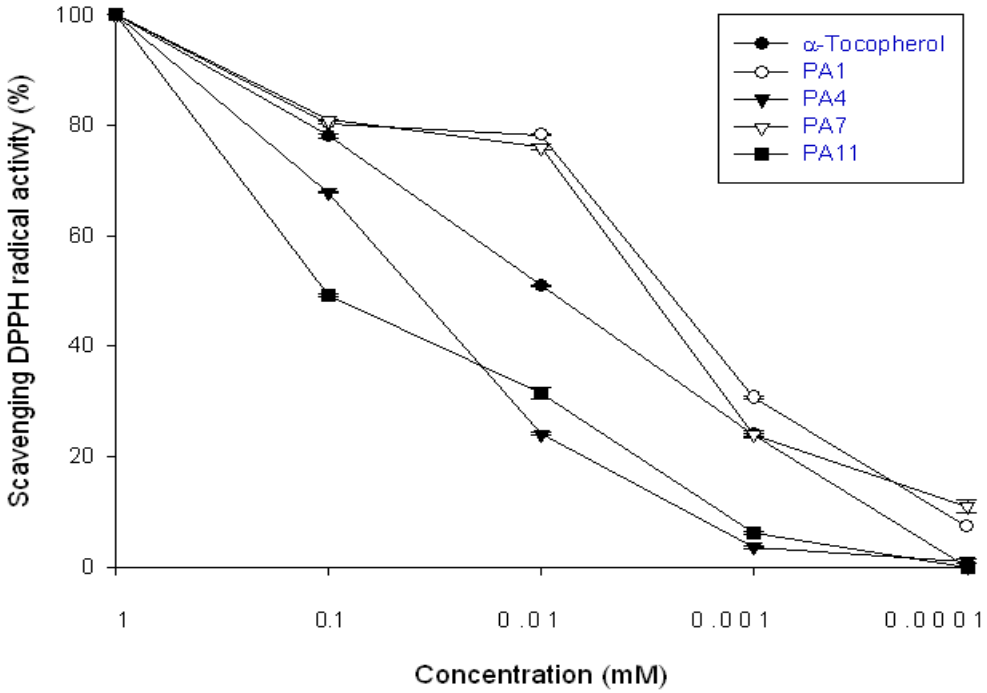

Fig. 1 □□□Selected compounds PA1, PA4, PA7 and PA11 showed a dose-dependent manner in scavenging activity of DPPH radical. Each point is expressed as mean± S.E.M. of triplicate.